AAS 13-937

OPTIMIZED FREE-RETURN TRAJECTORIES TO NEAR-EARTH ASTEROIDS VIA LUNAR FLYBY

Nicholas Bradley, Sonia Hernandez,[*] and Ryan P. Russell[†]

An algorithm is presented to generate an initial guess and converge a trajectory to reach a near-Earth asteroid in a fuel-optimal sense with emphasis on manned-mission risk reduction. The trajectory is designed such that the departing vehicle will return to Earth with no extra maneuvers, and incorporates a lunar flyby on the outbound segment to reduce fuel cost. The nominal mission departs the free-return trajectory to rendezvous with the asteroid for a minimum period of time before returning to Earth. The optimization scheme incorporates a full ephemeris model and analytical gradients for accurate convergence. The method is useful for fuel cost reduction of interplanetary trajectories in general that include a lunar flyby. An example case is presented to rendezvous with asteroid 2000 SG344 that departs Earth on 30 March 2028 and returns from the nominal mission on 24 March 2029 for a total mission cost of 3.850 km/s and duration of 359 days. The total cost of the mission is an improvement from previous work, and is comparable to patched conic rendezvous missions that do not incorporate a free-return segment.

INTRODUCTION

In recent decades, near-Earth asteroids (NEAs) have received significant attention as viable destinations for robotic and manned missions. There continues to be a growing amount of literature detailing trajectories from Earth to these primitive bodies. These largely consist of one-way rendezvous trajectories,[1–3] optimal rendezvous or flyby,[4–6] and destination selection algorithms.[7–10] The body of work on travel to NEAs has provided the community with many trajectory schemes to lower travel time, total mission ΔV (for impulsive transfers), or total fuel cost (for finite-thrust transfers). However, when a round-trip voyage is presented in the literature, the risk of engine failure or fuel loss is usually not considered. Works that address abort scenarios for deep space missions quite often place the focus on alternate trajectories that may be taken in the event of mission abort,[10,11] requiring the use of an engine that may not be able to provide the required capabilities in a critical scenario.

To address this risk, a precursor work has previously introduced the application of free-return trajectories (FRTs) to visit NEAs.[12] Similar to the trajectories used by the Apollo program to visit the Moon,[13] these FRTs provide a fuel-free return to Earth to partially mitigate the risk of catastrophic engine or fuel failure. If a failure occurs, the vehicle may remain on the trajectory and return to a

[*]Ph.D. Candidates, Department of Aerospace Engineering and Engineering Mechanics, The University of Texas at Austin, W.R. Woolrich Laboratories, 1 University Station, C0600, 210 E. 24th St., Austin TX 78712, USA; Student members AIAA and AAS. nick.bradley@utexas.edu and sonia.hernandez@utexas.edu

[†]Assistant Professor, Department of Aerospace Engineering and Engineering Mechanics, The University of Texas at Austin, W.R. Woolrich Laboratories, 1 University Station, C0600, 210 E. 24th St., Austin TX 78712, USA; Member AIAA and AAS. ryan.russell@austin.utexas.edu

re-entry state for safe return to Earth. If the mission is nominal, the vehicle may depart from the FRT in a ΔV-optimal sense to rendezvous with the destination NEA. Such trajectories have previously been studied for many applications,[14–19] but not for NEA mission risk mitigation.

This study investigates two further aspects of using an FRT to visit a NEA. First, and most notably, is the use of a lunar flyby to lower the overall mission ΔV cost. Lunar flybys are often used in interplanetary missions to lower total ΔV. By performing a flyby of the moon on the Earth departure leg, the mission achieves a lower cost than would be attainable by simply departing Earth with no flyby. Similar work has been previously presented by Hernandez and Barbee, showing how a lunar flyby may be used to improve fuel cost on a round-trip trajectory to a NEA.[20]

Secondly, the current work utilizes full ephemerides for the relevant bodies, and incorporates gravitational forces from the Earth, Moon, and Sun in all phases of the mission. Previously, the circular restricted three-body model was used, assuming that the Earth and Moon constituted a point-mass in a circular orbit around the Sun-Earth barycenter. With the improvement in dynamical model fidelity, the results presented here are more accurate than those previously supplied.

This paper is organized as follows: the Models section details the specific dynamics of the system, and gives a definition and background for a free-return trajectory. The Methods section is divided into three subsections. First, the Parameters and Constraints subsection introduces the free parameters and related constraints for the problem. Second, the Initial Guess subsection details the algorithm developed to provide an initial trajectory guess to the optimization algorithm. Finally, the Optimization subsection provides a description of the high-level algorithm for determining the ΔV-optimal trajectory to the selected NEA. The Results section presents an optimal trajectory to asteroid 2000 SG344, with an overall nominal mission ΔV of 3.850 km/s and nominal mission duration of 359 days. The Discussion section provides context for the results, comparing the numerical quantities to other mission types, and contains mention of future work.

MODEL

The problem as posed is to obtain a feasible round-trip trajectory to a target NEA which satisfies the following characteristics:

1. Incorporates a flyby of the Moon to reach the NEA
2. Incorporates an FRT after the lunar flyby
3. Is optimal in a ΔV cost sense for the nominal mission path
4. Includes a rendezvous with the NEA for a specified minimum time and returns to Earth on the nominal mission path

For purposes of this study, a free-return trajectory is defined as a path in space that returns the spacecraft to an Earth re-entry corridor with no deterministic maneuvers. That is, if the spacecraft is on an FRT, it will return to Earth with no further maneuvers required. The trajectory is not required to be periodic or to return to the same point in space as the one from which it departed the Earth. Specific departure and return flight path angles are not constrained in this study, but these may easily be added as requirements for specific mission designs.

A historical example of the use of FRTs comes from the Apollo program. The Apollo 8 spacecraft departed from a low-Earth orbit (LEO) and would have returned to Earth on a circumlunar trajectory had it not applied any further maneuvers.[13] A similar concept is used in this work. As soon as the

spacecraft departs from its LEO parking orbit, a purely ballistic trajectory with a lunar flyby will return it back to Earth. If an abort scenario is encountered, the spacecraft stays on the FRT instead of departing for rendezvous with the NEA.

The dynamics of the system include the point-mass gravitational influences of the Earth, Moon, and Sun at all times on the trajectory. Eq. (1) gives the full form of the equations of motion, with position vector $\mathbf{r}$ defined with respect to the Earth. The subscripts refer to Earth (e), the Sun (s), the Moon (m), and the spacecraft (sc), and a relative position is given with a double subscript, e.g. sc/s for the spacecraft with respect to Sun.

$$\ddot{\mathbf{r}} = -\frac{\mu_e}{r^3}\mathbf{r} - \mu_s\left(\frac{\mathbf{r}_{s/e}}{r_{s/e}^3} + \frac{\mathbf{r}_{sc/s}}{r_{sc/s}^3}\right) - \mu_m\left(\frac{\mathbf{r}_{m/e}}{r_{m/e}^3} + \frac{\mathbf{r}_{sc/m}}{r_{sc/m}^3}\right) \tag{1}$$

Since optimal rendezvous with the target NEA is desired on the nominal mission path, parameters associated with departing the FRT and rendezvousing with the asteroid are incorporated into the optimization scheme. Nominally, the spacecraft departs the FRT, performs a rendezvous with the asteroid for a finite amount of time, and departs for Earth return. The mission scheme is shown in illustrative form in Figure 1. Note that the Sun's gravity is part of the system dynamics, even though it is not shown in the figure. Maneuver $\Delta\mathbf{v}_0$ is performed to begin the mission. If an abort is necessary, the spacecraft naturally returns to Earth after lunar flyby. Nominally, $\Delta\mathbf{v}_c$ is performed to travel to the NEA. Finally, $\Delta\mathbf{v}_a$ completes the rendezvous, and $\Delta\mathbf{v}_d$ initiates the departure for return to Earth.

Also shown in Figure 1 are the patch points (white circles), which are described in more detail the Methods section. The direction of the arrows indicates direction of integration; e.g., the state at Earth return is integrated backward in time to the patch point at t_c. This is used in the paper for optimizing the trajectory using a multiple shooting method. Regardless of integration direction, the trajectories are all continuous and smooth in a forward-propagated direction.

The precursor work focused on the circular restricted three-body model (CRTBM) to calculate free-return trajectories.[12] In the current work, the dynamical model uses the full ephemerides for the Earth, the Moon, and the Sun. This gives a higher fidelity model, even while ignoring minor effects such as asteroid gravity, non-spherical gravitational terms, and non-gravitational forces.

The data for the ephemerides comes from JPL's SPICE toolkit, which uses the DE421 planetary ephemerides [i].

METHODS

Parameters and Constraints

To find an optimal solution, an initial guess algorithm is used to generate a reasonable set of parameters for the optimization algorithm to iterate. The optimizer operates on this set of parameters to satisfy equality and inequality constraints while minimizing a performance index. The relevant parameters ($\mathbf{X}_p$), inequality constraints ($\mathbf{d}$), and equality constraints ($\mathbf{c}$) are given in Eq. (2). Each vector is scaled by a diagonal weighting matrix ($\mathbf{W}_x$, $\mathbf{W}_d$, or $\mathbf{W}_c$) which is necessary for proper optimizer convergence.

[i] Data available from JPL at http://naif.jpl.nasa.gov/pub/naif/generic_kernels/spk/planets/

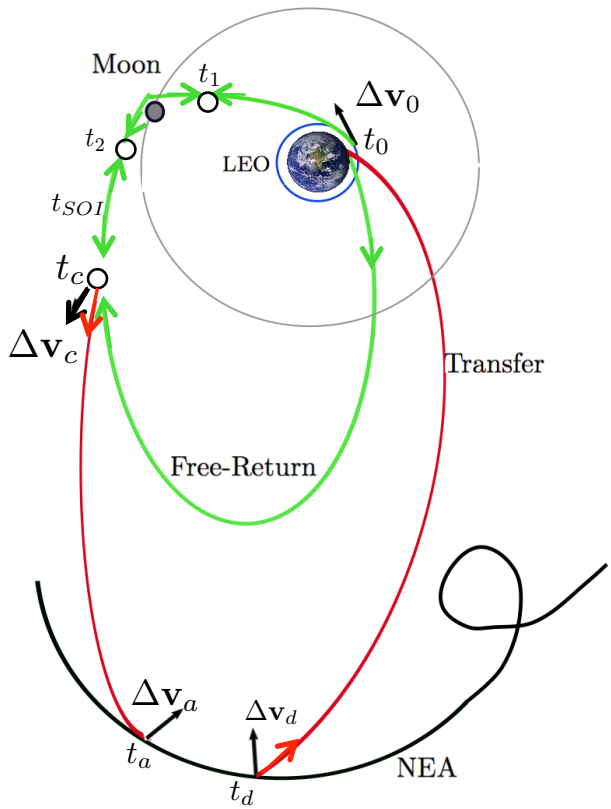

Figure 1: Conceptual diagram of mission segments and ΔV maneuvers.

$$\mathbf{X}_p = \mathbf{W}_x \begin{bmatrix} t_0 \\ t_m \\ t_{SOI} \\ t_c \\ t_a \\ t_d \\ t_{FR} \\ t_f \\ i_0 \\ \Omega_0 \\ \nu_0 \\ \phi_{SOI} \\ \phi_{FR} \\ \phi_f \\ \lambda_{SOI} \\ \lambda_{FR} \\ \lambda_f \\ \mathbf{r}_m \\ \Delta v_0 \\ \mathbf{v}_m \\ \mathbf{v}_{SOI} \\ \Delta\mathbf{v}_c \\ \mathbf{v}_{FR} \\ \mathbf{v}_f \end{bmatrix}_{36\times1} \qquad \mathbf{d} = \mathbf{W}_d \begin{bmatrix} t_0 \\ (t_m - t_0) - 0.5 \\ (t_{SOI} - t_m) - 0.5 \\ t_a - t_c \\ t_{FR} - t_c \\ t_f - t_d \\ (t_c - t_{SOI}) - t_{FR,min} \\ (t_d - t_a) - t_{stay,min} \\ t_{FR,max} - (t_{FR} - t_0) \\ |\mathbf{r}_m| - r_{flyby,min} \\ v_{return,max} - |\mathbf{v}_{FR}| \\ v_{return,max} - |\mathbf{v}_f| \end{bmatrix}_{12\times1} \geq \mathbf{0}$$

$$\mathbf{c} = \mathbf{W}_c \begin{bmatrix} \mathbf{r}(t_1)^+ - \mathbf{r}(t_1)^- \\ \mathbf{r}(t_2)^+ - \mathbf{r}(t_2)^- \\ \mathbf{r}(t_c)^+ - \mathbf{r}(t_c)^- \\ \mathbf{r}_{sc}(t_a) - \mathbf{r}_a(t_a) \\ \mathbf{r}_{sc}(t_d) - \mathbf{r}_a(t_d) \\ \mathbf{v}(t_1)^+ - \mathbf{v}(t_1)^- \\ \mathbf{v}(t_2)^+ - \mathbf{v}(t_2)^- \\ \mathbf{v}(t_c)^+ - \mathbf{v}(t_c)^- \end{bmatrix}_{24\times1} = \mathbf{0} \tag{2}$$

Earth departure occurs at time t_0 from a circular orbit at a specified altitude of 400 km described by the orbital elements i_0 (inclination), Ω_0 (right ascension), and ν_0 (true anomaly from ascending node). A maneuver $\Delta\mathbf{v}_0$ with magnitude Δv_0 is applied in the along-track orbit direction to begin traveling toward the Moon. The trajectory continues to the first patch point at time t_1, which is half a day prior to lunar flyby. Lunar close approach, or perilune, occurs at time t_m, with position $\mathbf{r}_m$ and velocity $\mathbf{v}_m$ relative to the moon. The time from Earth to perilune and perilune to the Moon's SOI must be at least half a day. This perilune state continues to the second patch point at time t_2, which is half a day after t_m.

A sphere of influence (SOI) is defined at a distance suitably far away from the Earth-Moon system where the individual effects of each body are diminished and the gravitational field becomes largely that of a single central body. Additionally, gravitational effects of the Sun begin to dominate those of the Earth-Moon. There are various ways of computing different definitions of the SOI's radius. For purposes of this work, the radius is selected to be 5×10^5 km from Earth's center. The exact definition of a "sphere of influence" is unimportant to the discussion; a suitably far distance for an intermediate state is all that is necessary.

The state associated with SOI passage occurs at time t_{SOI}, with velocity $\mathbf{v}_{SOI}$ and J2000 latitude and longitude of ϕ_{SOI} and λ_{SOI}, respectively. Note that latitude and longitude correspond to spherical coordinates in an Earth-centered J2000 reference frame. This state continues to the third patch point at time t_c, and the spacecraft is required to be on this segment for a certain minimum time $t_{FR,min}$. This time t_c is also the departure time for the nominal mission approach toward the NEA. An impulse $\Delta\mathbf{v}_c$ is applied, and rendezvous occurs at time t_a. The spacecraft must stay with the asteroid for a minimum time $t_{stay,min}$, and departs at time t_d.

Finally, two states are defined at Earth return: one for the FRT, and one for nominal mission return. These consist of the times (t_{FR} and t_f, respectively), latitude/longitude (ϕ_{FR}, λ_{FR} and ϕ_f, λ_f, respectively), and velocities ($\mathbf{v}_{FR}$ and $\mathbf{v}_f$, respectively).

Equality constraints at patch points are denoted as being either before (–) or after (+) the patch point. These patch points are schematically shown as white circles in Figure 1.

Initial guess

The optimization algorithm requires a suitable initial guess upon which to operate. This work uses concepts from two-body orbital mechanics, Lambert targeting, and patched conics to arrive at an appropriate initial guess. A high-level order of the initial guess routine is as follows:

1. Target lunar flyby to enter into FRT
2. Determine favorable NEA rendezvous time
3. Calculate Earth-return leg from NEA

Target lunar flyby The first segment is the lunar flyby into the free-return trajectory. One simple family of free-return trajectories consists of resonant single-period orbits that have the same period as the return body. In this case, a Sun-centered two-body orbit beginning at the Earth with a two-body period of one year will return near the Earth in a full dynamical system in approximately one year. In a patched conic sense, this behavior may be approximated by targeting a specific heliocentric departure speed from the Earth-Moon system. In the two-body model, if the spacecraft departing from Earth's position has the same speed as Earth, it will return to the same position after

one year. Therefore, the initial guess algorithm targets a heliocentric spacecraft speed at SOI equal to Earth's heliocentric speed. Because this is an initial guess routine, the exact heliocentric speed of the Earth-Moon barycenter does not need to be used, as the goal of the routine is to find a solution that is suitable for the optimizer.

The algorithm first calculates a two-body Earth-centered Lambert-targeted trajectory from low-Earth orbit to the Moon. With the arrival conditions at the Moon, a patched conic approach is taken to determine the post-flyby conditions corresponding to a choice of certain free parameters (described in detail below). The post-flyby state is propagated using Kepler's equation to the SOI, where the heliocentric speed is determined. The free parameters at lunar flyby are adjusted so that this speed corresponds to an FRT with a return period of one year. The algorithm used to determine the post-flyby conditions and Moon-centric close approach state is described in detail in Appendix A.

For the targeting routine, six free parameters ($\mathbf{p}$) are varied to target the single constraint (c) of heliocentric speed at SOI. Departure latitude and longitude around the Earth (ϕ_0, λ_0), time of flight to the Moon (TOF), Moon-centric latitude and longitude (ϕ_m, λ_m), and initial epoch (t_0) are all varied. These quantities are consolidated in Eq. (3). Figure 2 gives a graphical representation of the free parameters and the constraint locations.

$$\mathbf{p} = \begin{bmatrix} \phi_0 \\ \lambda_0 \\ TOF \\ \phi_m \\ \lambda_m \\ t_0 \end{bmatrix} \qquad c = |\mathbf{v}_{SOI}| - |\mathbf{v}_{Earth}| = 0 \tag{3}$$

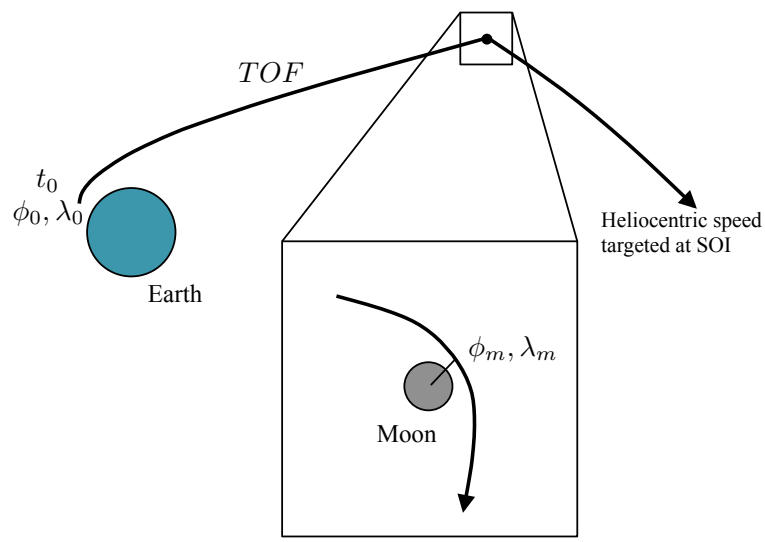

Figure 2: Conceptual diagram of target parameters for lunar flyby

The initial guess up to this point includes Earth departure, lunar flyby, and free-return generation to return to Earth. After the Earth departure and Moon flyby states have been calculated, the solution represents an initial guess to all segments of the full system except those involving asteroid

rendezvous and departure.

NEA rendezvous To obtain an initial guess for asteroid rendezvous, it is important to choose a reference epoch that contains reasonable relative positioning of the asteroid and Earth around the Sun. To find times of favorable geometries, the results from the Near-Eath Object Human Space Flight Accessible Targets Study (NHATS),[21] conducted by NASA's Near Earth Object program, are utilized. The study produced results for basic calculations of two-body Lambert targeted trajectories from the Earth to a large list of potential mission targets. By selecting a specific target NEA, a viable rendezvous epoch may be obtained by searching for a time period with a low relative total ΔV to rendezvous with the body in a heliocentric two-body sense. This epoch represents a time with favorable gemoetries for Earth-to-NEA missions.

Earth return leg Once a reasonable rendezvous and departure time are found, the final portion of the initial guess algorithm uses a heliocentric Lambert-targeting scheme and a differential correction method to calculate the return to Earth. The Lambert targeter calculates the velocities necessary to travel from the NEA to a massless Earth in a Sun-centered system. The state obtained from this step is then numerically propagated in a full gravitational model (including the Moon and Earth) from the NEA back to Earth. Since the two-body parameters are propagated in a full model, the trajectory will not reach the desired re-entry constraints at Earth. To correct this error, a differential correction scheme is initiated whereby a single component of the NEA departure velocity is varied to target a scalar perigee value of 7000 km. This targeting is accomplished using a state transition matrix (STM)-based Newton-Raphson differential correction algorithm.

The free parameter of the correction algorithm is a component of velocity at asteroid departure, and the function to be zeroed is $f = (|\mathbf{r}_{earth}| - 7000\ km)$. The first derivative of this function with respect to the ith component of velocity at the asteroid is related through the STM following Eq. (4), where the STM is denoted by $\mathbf{\Phi}$. The subscript indicates the first three rows (1:3) and the $3 + i^{th}$ column of the matrix, corresponding to the ith component of velocity at the asteroid.

$$df = \frac{d}{dv_i}\left(|\mathbf{r}_{earth}|\right) = \frac{\mathbf{r}_{earth}^{\top}}{|\mathbf{r}_{earth}|}\mathbf{\Phi}_{1:3,3+i} \tag{4}$$

After several iterations of the Newton-Raphson iteration scheme, the error in radius at Earth return decreases to the order of tens of kilometers. At this point, the state at Earth return is used for the corresponding states and times in the end-to-end optimization scheme.

Optimization

The optimization of the parameters from the initial guess algorithm is performed using a sequential quadratic programming algorithm VF13 in Fortran from the Harwell Subroutine Library.[22] This prepackaged algorithm operates on a set of parameters to satisfy a set of inequality and equality constraints. For this specific problem, these quantities are given in Eq. (2). The routine also minimizes a scalar cost function J, which is the sum of all the deterministic velocity maneuvers. The cost function is given in Eq (5).

$$J = \Delta v_0 + |\Delta \mathbf{v}_c| + |(\mathbf{v}_a(t_a) - \mathbf{v}_{sc}(t_a))| + |(\mathbf{v}_{sc}(t_d) - \mathbf{v}_a(t_d))| \tag{5}$$

In order, the terms represent the magnitude of the initial impulse to leave Earth, the magnitude of the impulse to leave the FRT, the magnitude of the difference between the NEA's velocity and

the spacecraft velocity at rendezvous, and the magnitude of the difference between the spacecraft's velocity and the NEA's velocity at departure. In all, there are four impulsive maneuvers which comprise the cost function.

The optimization routine requires the gradients of the cost function and constraints with respect to the parameters of the system. All gradients have been calculated analytically, which lead to fast and accurate computation. Note that these gradients, deemed "analytical," are dependent on numerically propagating the state transition matrix along with the state of the spacecraft on the trajectory.

The gradients are calculated by solving Eq. (6), where the initial condition $\mathbf{I}$ is the identity matrix.

$$\dot{\mathbf{\Phi}} = \frac{\partial f(\mathbf{x})}{\partial \mathbf{x}} \mathbf{\Phi} \ , \qquad \mathbf{x} = \begin{bmatrix} \mathbf{r} \\ \mathbf{v} \end{bmatrix}_{6\times 1} \ , \quad f(\mathbf{x}) = \begin{bmatrix} \mathbf{v} \\ \ddot{\mathbf{r}} \end{bmatrix}_{6\times 1} \ , \quad \mathbf{\Phi}(0,0) = \mathbf{I}_{6\times 6} \tag{6}$$

To compute the gradients, Eq. (7) is used to relate the differentials of the state $\mathbf{x}$ at any time t_{i+1} to any other time t_i.[23]

$$d\mathbf{x}_{i+1}^{+} = \mathbf{\Phi}(t_{i+1}, t_i) \left[d\mathbf{x}_i^{-} + d\Delta\mathbf{x}_i - \dot{\mathbf{x}}_i^{+} dt_i \right] + \dot{\mathbf{x}}_{i+1}^{-} dt_{i+1} + d\Delta\mathbf{x}_{i+1} \tag{7}$$

Therefore, given the state and the STM between any two times, the full Jacobian matrix of first order partial derivatives may be obtained for the optimization routine. The accuracy of the Jacobian is limited primarily to the accuracy of the numerical solution of the differential equation given in Eq. (6). A discussion of this propagation and the full form of the gradients for the cost function and inequality constraints are found in Appendix B. Because of the number of non-zero gradients of equality constraints, these are omitted for brevity.

Upon convergence, the trajectory is 1) feasible, in that it satisfies all constraints, and 2) locally optimal, in that the cost function is at a local minimum at the converged set of parameters. Of course, there may exist other optima and an overall global optimum. Converging on these other solutions depends on the choice of initial guess and various optimizer settings, such as maximum step size and convergence criteria.

RESULTS

An example result is shown here for NEA 2000 SG344. Relevant optimizer parameters are given in Table 1 for the VF13 optimizer for Fortran [i]. Non-identity constraint scaling is explicitly stated, and it should be noted that the parameters were initially scaled to the order of unity. The algorithm was written in Fortran 90 and compiled using the GNU compiler `gfortran` running on a MacBook Pro with a 2.53 GHz Intel Core i5 processor and 4GB of RAM.

The NEA 2000 SG344 is known to be a highly accessible asteroid, because its orbit is very similar to Earth's orbit around the Sun; the semimajor axis is 0.978 AU, the eccentricity is 0.067, and the inclination with respect to the ecliptic is 0.111 degrees[ii]. Because its orbit is so similar to the Earth, a rendezvous mission typically requires a relatively small ΔV.

Using the initial guess and optimization algorithms described, a locally optimal fully-continuous solution was found with a total ΔV cost of 3.850 km/s from LEO to Earth return on the nominal

[i] The code package for VF13 may be obtained from http://www.hsl.rl.ac.uk/archive/

[ii] Data available at http://neo.jpl.nasa.gov/nhats/ [retrieved 23 Jul. 2013]. Note that these are approximations to instantaneous values for Epoch 2456400.5

Table 1: Optimizer parameters for VF13

Parameter	Value
Cost function convergence tolerance	1.0×10^{-3}
Eq. constraint scaling ($\mathbf{r}$)	1.0×10^{-6}
Eq. constraint scaling ($\mathbf{v}$)	1.0×10^{-3}
Ineq. constraint scaling (t_0)	1.0×10^{-6}
Ineq. constraint scaling ($\lvert\mathbf{r}_m\rvert$)	1.0×10^{-4}
Ineq. constraint scaling ($\lvert\mathbf{v}_{FR}\rvert$)	1.0×10^{-3}
Ineq. constraint scaling ($\lvert\mathbf{v}_f\rvert$)	1.0×10^{-3}

mission path. The initial LEO orbit is at an altitude of 400 km, which is the same initial altitude used in the NHATS study. Table 2 contains the relevant data for the converged mission. These results were independently verified by using the mission design software tool GMAT, developed by NASA's Goddard Spaceflight Center [i]. The relevant inequality constraint parameters are given in Table 3; a notable constraint is that the total mission time for the FRT must be less than one year. The minimum perilune radius corresponds to an altitude of 100 km above a spherical Moon. The spacecraft returns to a radius of 7000 km from the Earth's center.

Table 2: Converged results for 2000 SG344 rendezvous

Parameter	Description	Optimal value
t_0 (JD)	Earth departure date	2461861.237 (30 Mar 2028)
t_m (JD)	Moon close approach date	2461864.519 (03 Apr 2028)
t_c (JD)	FRT departure date	2461879.846 (18 Apr 2028)
t_a (JD)	NEA arrival date	2462032.154 (17 Sep 2028)
t_d (JD)	NEA departure date	2462042.154 (27 Sep 2028)
t_{FR} (JD)	FRT Earth-return date	2462208.346 (12 Mar 2029)
t_f (JD)	Nominal Earth-return date	2462219.836 (24 Mar 2029)
$\lvert h_m\rvert$ (km)	Perilune altitude	206.595
Δv_0 (km/s)	Earth departure impulse	3.087
Δv_c (km/s)	FRT departure impulse	0.127
Δv_a (km/s)	NEA arrival impulse	0.375
Δv_d (km/s)	NEA departure impulse	0.260
J	**Total ΔV cost**	**3.850 km/s**

Final equality constraint magnitudes for the converged solution are given in Table 4. Each constraint is denoted as $\mathbf{c}_i$ for the ith vector equality constraint from Eq. (2).

Figure 3 shows the full converged set of trajectories in the J2000 XY plane and from an oblique perspective, centered at the Earth's center of mass. Figure 4 shows a close-up of the behavior in the Earth-Moon vicinity. Note that the trajectory performs an unenforced flyby of the Moon upon nominal return. A time history of the spacecraft's distance from Earth is given in Figure 5.

[i] GMAT is open-source software, available at http://gmat.gsfc.nasa.gov

Table 3: Inequality constraint parameters

Parameter	Description	Value
$t_{FR,min}$	Min. time to stay on FRT before departing	14.0 days
$t_{stay,min}$	Min. time to stay rendezvoused to NEA	10.0 days
$t_{FR,max}$	Max. time from t_0 to t_{FR}	365.0 days
$r_{flyby,min}$	Min. perilune radius	1838.0 km
$v_{return,max}$	Max. speed at Earth return (7000 km)	11.652 km/s

Table 4: Equality constraint magnitudes at convergence

Eq. constr.	Mag. at convergence	Units
$\mathbf{c}_1$	2.5×10^{-2}	km
$\mathbf{c}_2$	6.8×10^{-3}	km
$\mathbf{c}_3$	4.0×10^{0}	km
$\mathbf{c}_4$	2.8×10^{-1}	km
$\mathbf{c}_5$	3.3×10^{1}	km
$\mathbf{c}_6$	5.4×10^{-4}	m/s
$\mathbf{c}_7$	1.8×10^{-3}	m/s
$\mathbf{c}_8$	8.2×10^{-4}	m/s

DISCUSSION

The example trajectory found to rendezvous with NEA 2000 SG344 represents a significant decrease in ΔV cost over a solution found with no lunar flyby.[12] Although the comparison cannot be exact since the previous work used a restricted dynamical model and a slightly different departure date from the previous work, the decrease in ΔV is quite pronounced. The previous work found a total cost of 5.307 km/s with the same cost function and no lunar flyby. The current work represents a decrease of 1.457 km/s (27.5%) by utilizing lunar flybys in a more accurate dynamical system.

Additionally, the risk mitigation factor of using an FRT is preserved, even if some mission risk is added by performing a close flyby of the Moon. Upon departure from the low-Earth parking orbit, the spacecraft follows a ballistic trajectory around the Moon and back to Earth. While small trajectory correction maneuvers would be necessary on an actual mission to target specific lunar flyby parameters, the trajectory can be viewed as a completely ballistic FRT to first order.

As a further point of comparison, the example trajectory may be compared to a round-trip heliocentric two-body trajectory found using the NHATS database.[21] For a similar range of dates, the NHATS study computed Lambert arcs from a LEO orbit of 400 km altitude to the NEA and back to Earth re-entry. For 2000 SG344, the study found an overall minimum ΔV of 3.556 km/s for a round-trip mission duration of 354 days. Imposing the constraint of a free-return and propagating in a full dynamical model in the current work imposes an increase of only 294 m/s.

It may also be assumed that the initial impulse to depart from low-Earth orbit can come from a launch vehicle's secondary or tertiary motor. Many launch vehicles currently carry the capability

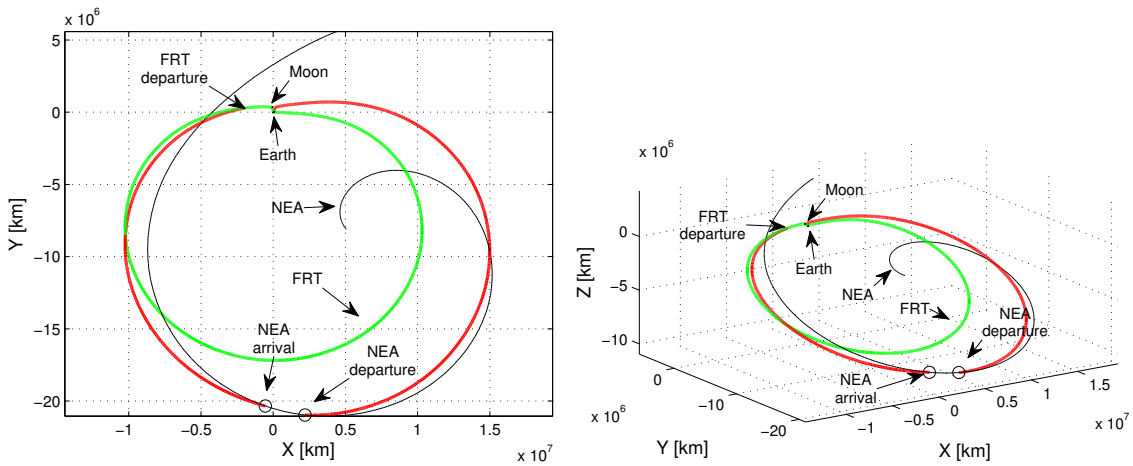

(a) XY plane.

(b) Oblique view.

Figure 3: Full converged trajectory set to 2000 SG244 in an Earth-centered J2000 frame.

to inject a spacecraft on an Earth-departure orbit so that the spacecraft itself is not responsible for carrying the fuel to perform the departure ΔV. If this capability is assumed for this example, the spacecraft must only perform a total ΔV of 762 m/s, which is quite feasible.

The FRT return and nominal return to Earth satisfy inequality constraints imposed to limit the entry speed into Earth's atmosphere. At a return radius of 7000 km, the spacecraft is constrained to have a speed of no more than 11.652 km/s. In a two-body sense, this corresponds to a speed of 12 km/s at an altitude of 150 km, which represents a common Earth re-entry upper limit on speed. The solution meets the constraint by a comfortable margin, with the FRT return at a speed of 10.712 km/s and the nominal return at a speed of 10.612 km/s. The return geometry is shown in Figure 6(a), which depicts Earth departure and both return trajectories. Interestingly, the trajectory performs a flyby of the moon on the nominal return leg in addition to the departure leg. Although this behavior is not enforced by the constraints in the optimizer, the return flyby reduces total ΔV and could be used to lower the incoming velocity for re-entry on the nominal mission. A Moon-centered figure of the outbound and inbound legs is shown in Figure 6(b), depicting the flyby characteristics in a Moon-centered J2000 frame.

The converged lunar flyby geometry on the outbound leg satisfies the inequality constraints imposed. The constraint from Table 3 limits the lunar flyby altitude to 100 km. The final converged trajectory gives a flyby altitude of 206.595 km.

Future work will involve improvement to the initial guess algorithm to create a more robust way of determining an appropriate input to the optimization algorithm. Resulting methods will be applied to more near-Earth objects to determine the best candidates for this type of mission. A grid search on other parameters may also be conducted on a single destination to determine a more globally optimal solution in terms of ΔV.

CONCLUSION

A method is presented to calculate an end-to-end round-trip trajectory to rendezvous with a near-Earth asteroid. This trajectory utilizes free-return trajectory capabilities for risk reduction in the

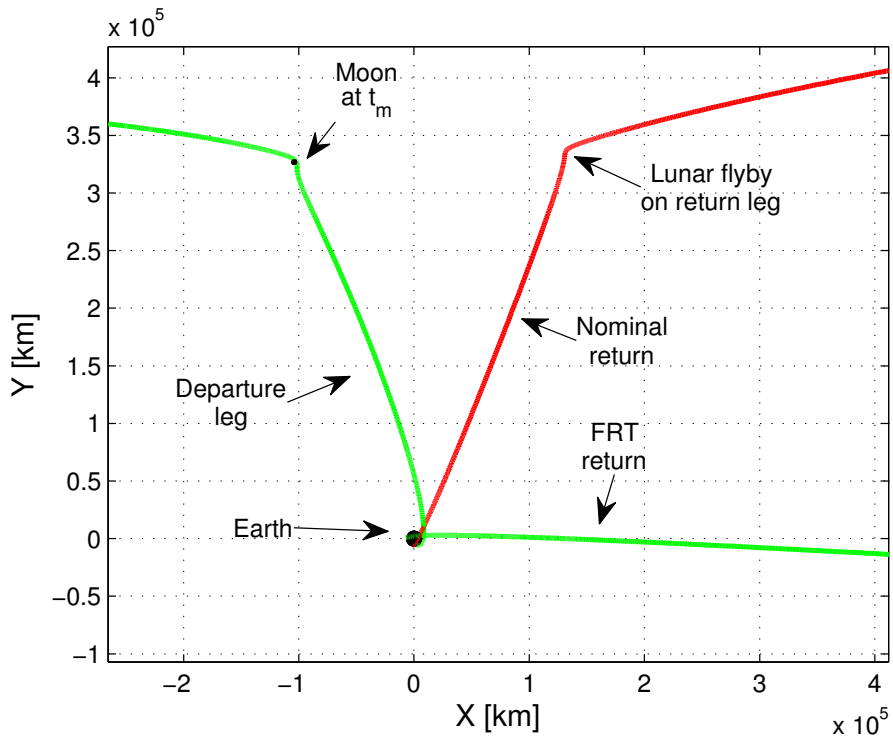

Figure 4: Trajectory behavior in the Earth-Moon system.

event of an abort scenario on a manned spacecraft. To lower ΔV cost, the algorithm makes use of a lunar flyby upon Earth departure to embark upon the free-return trajectory. The spacecraft departs the free-return in a ΔV-optimal sense, rendezvouses with the asteroid, and departs from the asteroid to return to Earth. Although a lunar flyby potentially increases risk due to the navigational challenges introduced to the mission, the ΔV savings are appreciable, and the total cost is comparable to a two-body rendezvous calculation with no free return capability. The flyby segment makes the algorithm useful to general interplanetary trajectories that incorporate a lunar flyby to lower total fuel cost.

An example trajectory is shown with near-Earth asteroid 2000 SG344. The total optimized cost for the mission is 3.850 km/s, which represents an improvement of nearly 30% over a similar trajectory using a free-return that was previously found. This figure is comparable to the cost of 3.556 km/s found in the NHATS study by using two-body patched conics without free-return capabilities. Mission designers must weigh the risk of introducing a lunar flyby compared to the benefit of lowering the total ΔV for this type of mission. The presence of a free return trajectory serves to lower the overall risk of these rendezvous missions in comparison to other simple targeting procedures.

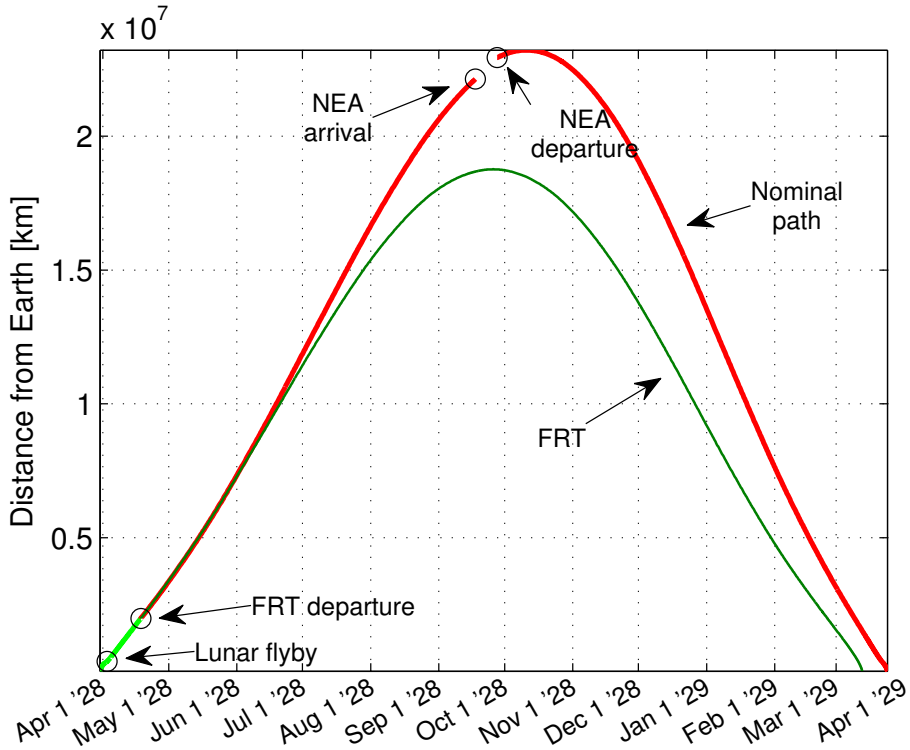

Figure 5: Spacecraft distance from Earth for FRT and nominal mission.

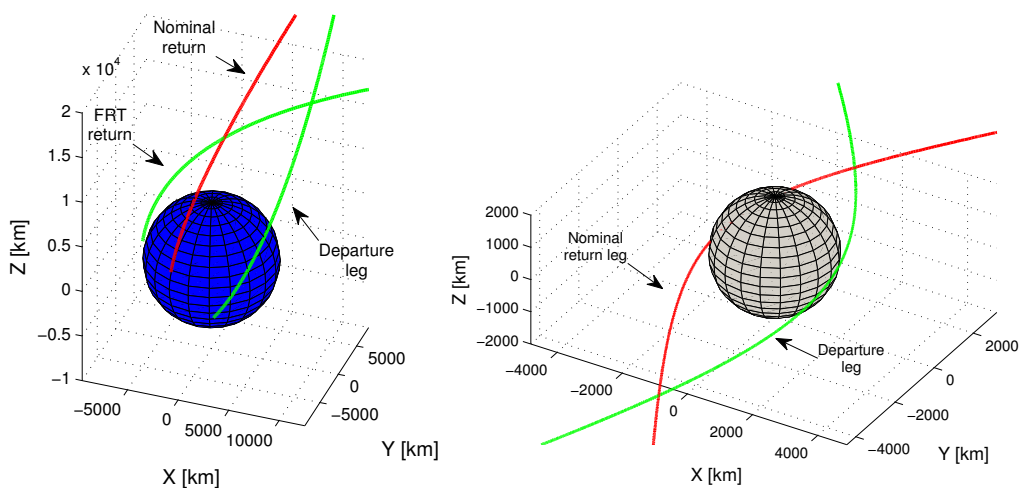

(a) Earth-centric departure and return.

(b) Moon-centric departure and return flybys.

Figure 6: Trajectory geometry at Earth and Moon.

APPENDIX A: LUNAR FLYBY PARAMETERS

The targeting algorithm described in the Initial Guess section iterates on two spherical angles (ϕ, λ) at lunar flyby. The following routine is used to determine the state at lunar flyby given these two

angles and the incoming velocity vector of the spacecraft.

1. Calculate the incoming hyperbolic excess velocity from the Earth-to-Moon segment:

$$\mathbf{v}_\infty^- = \mathbf{v}_{sc}^- - \mathbf{v}_{moon} \tag{8}$$

2. Calculate the flyby direction and angular momentum direction with respect to the moon:

$$\hat{\mathbf{r}}_p = \begin{bmatrix} \cos\phi\cos\lambda \\ \cos\phi\sin\lambda \\ \sin\phi \end{bmatrix}, \qquad \hat{\mathbf{h}} = \frac{\hat{\mathbf{r}}_p \times \mathbf{v}_\infty^-}{\left|\hat{\mathbf{r}}_p \times \mathbf{v}_\infty^-\right|} \tag{9}$$

3. Find the turning angle δ by which the velocity vector is rotated through the flyby:

$$\delta = \pi - 2\cos^{-1}\left(\frac{\hat{\mathbf{r}}_p \cdot \mathbf{v}_\infty^-}{\left|\mathbf{v}_\infty^-\right|}\right) \tag{10}$$

4. Using an axis-angle rotation scheme, rotate the $\mathbf{v}_\infty^-$ vector about the $\hat{\mathbf{h}}$ vector by angle δ to obtain $\mathbf{v}_\infty^+$.

5. With angle δ, the magnitude of the close approach flyby radius may be found:

$$e = \frac{1}{\sin(\delta/2)} \quad \Rightarrow \quad |\mathbf{r}_p| = \frac{\mu_{moon}(e-1)}{\left|\mathbf{v}_\infty^-\right|^2} \tag{11}$$

6. Obtain the energy E, semimajor axis a, and angular momentum h magnitudes of the flyby:

$$E = \frac{\left|\mathbf{v}_\infty^-\right|^2}{2}, \qquad a = \frac{-\mu_{moon}}{2E}, \qquad h = \sqrt{\mu_{moon} a(1-e^2)} \tag{12}$$

7. Finally, obtain the speed at close approach from the close approach distance and angular momentum:

$$|\mathbf{v}_p| = \frac{h}{|\mathbf{r}_p|} \quad \Rightarrow \quad \boxed{\mathbf{r}_p = |\mathbf{r}_p| \begin{bmatrix} \cos\phi\cos\lambda \\ \cos\phi\sin\lambda \\ \sin\phi \end{bmatrix}, \quad \mathbf{v}_p = |\mathbf{v}_p| \frac{\mathbf{v}_\infty^+ + \mathbf{v}_\infty^-}{\left|\mathbf{v}_\infty^+ + \mathbf{v}_\infty^-\right|}} \tag{13}$$

APPENDIX B: ANALYTIC GRADIENTS

For the sequential quadratic programming optimization routine, these gradients are calculated using the variational equations given in Eq. (7) with the numerical integration of the state transition matrix given in Eq. (6). Each term in the equality and inequality constraint vectors ($\mathbf{c}$ and $\mathbf{d}$ in Eq. (2), respectively) is given a subscript here for brevity; e.g. the nth term listed in the inequality constraint vector is shown here as $\mathbf{d}_n$.

Additionally, the state transition matrix is divided into four 3×3 submatrices, so that the state transition matrix from t_a to t_b is denoted as:

$$\mathbf{\Phi}_{ba} = \left[\begin{array}{c|c} \mathbf{A}_{ba} & \mathbf{B}_{ba} \\ \hline \mathbf{C}_{ba} & \mathbf{D}_{ba} \end{array}\right]$$

Analytical gradients are given in the following equations. All gradients are given for the cost function, and non-zero gradients are given only for the inequality constraints. Because of the number of non-zero gradients of equality constraints, these are omitted for brevity. Define $\Delta\mathbf{v}_a$ as the vector difference between the asteroid and the spacecraft at t_a and $\Delta\mathbf{v}_d$ as the vector difference between the asteroid and the spacecraft at t_d. Define $\mathbf{g}$ as the acceleration vector at a given time.

Cost function gradients

$$\frac{\partial J}{\partial t_0} = 0 \qquad \frac{\partial J}{\partial t_m} = 0 \qquad \frac{\partial J}{\partial t_{SOI}} = \frac{\Delta\mathbf{v}_a^\top}{\Delta v_a}\left(\mathbf{C}_{as}\mathbf{v}_{SOI} + \mathbf{D}_{as}\mathbf{g}(t_{SOI})\right)$$

$$\frac{\partial J}{\partial t_c} = -\frac{\Delta\mathbf{v}_a^\top}{\Delta v_a}\left(\mathbf{C}_{ac}\left(\mathbf{v}^-(t_c) - \mathbf{v}^+(t_c)\right)\right) \qquad \frac{\partial J}{\partial t_a} = \frac{\Delta\mathbf{v}_a^\top}{\Delta v_a}\left(\mathbf{g}_a(t_a) - \mathbf{g}_{sc}(t_a)\right)$$

$$\frac{\partial J}{\partial t_d} = \frac{\Delta\mathbf{v}_d^\top}{\Delta v_d}\left(\mathbf{g}_{sc}(t_d) - \mathbf{g}_a(t_d)\right) \qquad \frac{\partial J}{\partial t_F R} = 0 \qquad \frac{\partial J}{\partial t_f} = -\frac{\Delta\mathbf{v}_d^\top}{\Delta v_d}\left(\mathbf{C}_{df}\mathbf{v}_f + \mathbf{D}_{df}\mathbf{g}(t_f)\right)$$

$$\frac{\partial J}{\partial i_0} = 0 \qquad \frac{\partial J}{\partial \Omega_0} = 0 \qquad \frac{\partial J}{\partial \nu_0} = 0$$

$$\frac{\partial J}{\partial \phi_{SOI}} = \frac{\Delta\mathbf{v}_a^\top}{\Delta v_a}\left(-\mathbf{C}_{as} r_{SOI}\begin{bmatrix} -\cos\lambda_{SOI}\sin\phi_{SOI} \\ -\sin\lambda_{SOI}\sin\phi_{SOI} \\ \cos\phi_{SOI} \end{bmatrix}\right) \qquad \frac{\partial J}{\partial \phi_{FR}} = 0$$

$$\frac{\partial J}{\partial \phi_f} = \frac{\Delta\mathbf{v}_d^\top}{\Delta v_d}\left(\mathbf{C}_{df} r_f\begin{bmatrix} -\cos\lambda_f\sin\phi_f \\ -\sin\lambda_f\sin\phi_f \\ \cos\phi_f \end{bmatrix}\right)$$

$$\frac{\partial J}{\partial \lambda_{SOI}} = \frac{\Delta\mathbf{v}_a^\top}{\Delta v_a}\left(-\mathbf{C}_{as} r_{SOI}\begin{bmatrix} -\sin\lambda_{SOI}\cos\phi_{SOI} \\ \cos\lambda_{SOI}\cos\phi_{SOI} \\ 0 \end{bmatrix}\right) \qquad \frac{\partial J}{\partial \lambda_{FR}} = 0$$

$$\frac{\partial J}{\partial \lambda_f} = \frac{\Delta\mathbf{v}_d^\top}{\Delta v_d}\left(\mathbf{C}_{df} r_f\begin{bmatrix} -\sin\lambda_f\cos\phi_f \\ \cos\lambda_f\cos\phi_f \\ 0 \end{bmatrix}\right) \qquad \frac{\partial J}{\partial \mathbf{r}_m} = 0$$

$$\frac{\partial J}{\partial \Delta v_0} = 1 \qquad \frac{\partial J}{\partial \mathbf{v}_m} = \mathbf{0}_{3\times 1} \qquad \frac{\partial J}{\partial \mathbf{v}_{SOI}} = -\frac{\Delta\mathbf{v}_a^\top}{\Delta v_a}\mathbf{D}_{as}$$

$$\frac{\partial J}{\partial \Delta\mathbf{v}_c} = \frac{\Delta\mathbf{v}_c^\top}{\Delta v_c} - \frac{\Delta\mathbf{v}_a^\top}{\Delta v_a}\mathbf{D}_{ac} \qquad \frac{\partial J}{\partial \mathbf{v}_{FR}} = \mathbf{0}_{3\times 1} \qquad \frac{\partial J}{\partial \mathbf{v}_f} = \frac{\Delta\mathbf{v}_d^\top}{\Delta v_d}\mathbf{D}_{df}$$

Inequality constraint gradients

$$\frac{\partial \mathbf{d}_1}{\partial t_0} = 1 \qquad \frac{\partial \mathbf{d}_2}{\partial t_0} = -1 \qquad \frac{\partial \mathbf{d}_2}{\partial t_m} = 1 \qquad \frac{\partial \mathbf{d}_3}{\partial t_m} = -1 \qquad \frac{\partial \mathbf{d}_3}{\partial t_{SOI}} = 1$$

$$\frac{\partial \mathbf{d}_4}{\partial t_c} = -1 \qquad \frac{\partial \mathbf{d}_4}{\partial t_a} = 1 \qquad \frac{\partial \mathbf{d}_5}{\partial t_c} = -1 \qquad \frac{\partial \mathbf{d}_5}{\partial t_{FR}} = 1 \qquad \frac{\partial \mathbf{d}_6}{\partial t_d} = -1 \qquad \frac{\partial \mathbf{d}_6}{\partial t_f} = 1$$

$$\frac{\partial \mathbf{d}_7}{\partial t_{SOI}} = -1 \qquad \frac{\partial \mathbf{d}_7}{\partial t_c} = 1 \qquad \frac{\partial \mathbf{d}_8}{\partial t_a} = -1 \qquad \frac{\partial \mathbf{d}_8}{\partial t_d} = 1 \qquad \frac{\partial \mathbf{d}_9}{\partial t_0} = 1 \qquad \frac{\partial \mathbf{d}_9}{\partial t_{FR}} = -1$$

$$\frac{\partial \mathbf{d}_{10}}{\partial \mathbf{r}_m} = \frac{\mathbf{r}_m^\top}{r_m} \qquad \frac{\partial \mathbf{d}_{11}}{\partial \mathbf{v}_{FR}} = -\frac{\mathbf{v}_{FR}^\top}{v_{FR}} \qquad \frac{\partial \mathbf{d}_{12}}{\partial \mathbf{v}_f} = -\frac{\mathbf{v}_f^\top}{v_f}$$

REFERENCES

[1] Y. Chen, H. Baoyin, and J. Li, "Design and Optimization of a Trajectory for Moon Departure Near Earth Asteroid Exploration," *Science China Physics, Mechanics and Astronomy*, Vol. 54, No. 4, 2011, pp. 748–755.

[2] G. Mengali and A. Quarta, "Rapid Solar Sail Rendezvous Missions to Asteroid 99942 Apophis," *Journal of Spacecraft and Rockets*, Vol. 46, No. 1, 2009, pp. 134–140.

[3] E. Perozzi, A. Rossi, and G. Valsecchi, "Basic Targeting Strategies for Rendezvous and Flyby Missions to the Near-Earth Asteroids," *Planetary and Space Science*, Vol. 49, 2001, pp. 3–22.

[4] C. Colombo, M. Vasile, and G. Radice, "Optimal low-thrust trajectories to asteroids through an algorithm based on differential dynamic programming," *Celestial Mechanics and Dynamical Astronomy*, Vol. 105, No. 1–3, 2009, pp. 75–112.

[5] B. Conway, "Optimal Low-Thrust Interception of Earth-Crossing Asteroids," *Journal of Guidance, Control, and Dynamics*, Vol. 20, No. 5, 1997, pp. 995–1002.

[6] S. Park and K. Choi, "Optimal Low-Thrust Intercept/Rendezvous Trajectories to Earth-Crossing Objects," *Journal of Guidance, Control, and Dynamics*, Vol. 28, No. 5, 2005, pp. 1049–1055.

[7] D. Adamo, J. Giorgini, A. Abell, and R. Landis, "Asteroid Destinations Accessible for Human Exploration: A Preliminary Survey in Mid-2009," *Journal of Spacecraft and Rockets*, Vol. 47, No. 6, 2010, pp. 994–1002.

[8] C. Lau and N. Hulkower, "Accessibility of near-earth asteroids," *Journal of Guidance*, Vol. 10, No. 3, 1987, pp. 225–232.

[9] E. Shoemaker and E. Helin, "Earth-approaching asteroids as targets for exploration," *NASA N78-29022*, 1978.

[10] A. Zimmer and E. Messerschmid, "Going beyond: Target selection and mission analysis of human exploration missions to Near-Earth Asteroids," *Acta Astronautica*, Vol. 69, No. 11–12, 2011, pp. 1096–1109.

[11] P. Tartabini, S. Striepe, and R. Powell, "Abort Options for Potential Mars Missions," *Journal of Spacecraft and Rockets*, Vol. 31, No. 4, 1994, pp. 543–549.

[12] N. Bradley and C. Ocampo, "Optimal Free-Return Trajectories to Near-Earth Asteroids," *Journal of Guidance, Control, and Dynamics*, Vol. 36, No. 5, 2013, pp. 1346–1355.

[13] "Apollo 8 Press Kit," 1968. National Aeronautics and Space Administration, release 68-208.

[14] M. Jesick and C. Ocampo, "Automated Generation of Symmetric Lunar Free-Return Trajectories," *Journal of Guidance, Control, and Dynamics*, Vol. 34, No. 1, 2011, pp. 98–106.

[15] M. Jesick and C. Ocampo, "Optimal Lunar Orbit Insertion from a Variable Symmetric Free-Return Trajectory," *Journal of Guidance, Control, and Dynamics*, Vol. 34, No. 6, 2011, pp. 1867–1875.

[16] D. Landau and J. Longuski, "Trajectories for Human Missions to Mars, Part 1: Impulsive Transfers," *Journal of Spacecraft and Rockets*, Vol. 43, 2006, pp. 1035–1042.

[17] Q. Luo, J. Yin, and C. Han, "Design of Earth-Moon Free-Return Trajectories," *Journal of Guidance, Control, and Dynamics*, Vol. 36, No. 1, 2013, pp. 263–271.

[18] A. Meile, T. Wang, and S. Mancuso, "Optimal Free-Return Trajectories for Moon Missions and Mars Missions," *The Journal of the Astronautical Sciences*, Vol. 28, No. 2–3, 2000, pp. 183–206.

[19] M. Patel, J. Longuski, and J. Sims, "Mars Free Return Trajectories," *Journal of Spacecraft and Rockets*, Vol. 35, No. 3, 1998, pp. 350–354.

[20] S. Hernandez and B. Barbee, "Design of Round-Trip Trajectories to Near-Earth Asteroids Utilizing a Lunar Flyby," *Proc. 21st AAS/AIAA Space Flight Mechanics Meeting, New Orleans, Louisiana*, 2011.

[21] "Near-Earth Object Human Space Flight Accessible Targets Study (NHATS)," National Aeronautics and Space Administration. Results accessible on-line at `http://neo.jpl.nasa.gov/nhats/`. Accessed 1 Nov, 2012.

[22] "VF13," Harwell Subroutine Library Archive. Oxfordshire, England, 2001.

[23] C. Ocampo and J. Munoz, "Variational Equations for a Generalized Spacecraft Trajectory Model," *Journal of Guidance, Control, and Dynamics*, Vol. 33, No. 5, 2010, pp. 1615–1622.